







# Engineered electrospun polyurethane and castor oil nanocomposite scaffolds for cardiovascular applications

Saravana Kumar Jaganathan<sup>1,2,3,\*</sup> , Mohan Prasath Mani<sup>4</sup> ,  
Manikandan Ayyar<sup>5</sup> , and Eko Supriyanto<sup>4</sup> 

<sup>1</sup>Department for Management of Science and Technology Development, Ton Duc Thang University, Ho Chi Minh City, Vietnam

<sup>2</sup>Faculty of Applied Sciences, Ton Duc Thang University, Ho Chi Minh City, Vietnam

<sup>3</sup>IJN-UTM Cardiovascular Engineering Centre, Faculty of Biosciences and Medical Engineering, Universiti Teknologi Malaysia, 81300 Skudai, Johor, Malaysia

<sup>4</sup>Faculty of Biosciences and Medical Engineering, Universiti Teknologi Malaysia, 81300 Skudai, Johor, Malaysia

<sup>5</sup>Department of Chemistry, Bharath Institute of Higher Education and Research, Bharath University, Chennai, Tamil Nadu 600073, India

Received: 28 February 2017

Accepted: 9 June 2017

Published online:  
19 June 2017

© Springer Science+Business  
Media, LLC 2017

## ABSTRACT

Design of scaffolds with natural substances holds potential in several cardiovascular applications. In this study, we have fabricated scaffold using the electrospinning technique with blends of PU and castor oil. The characterization was performed using scanning electron microscopy (SEM), Fourier transform and infrared spectroscopy (FTIR), thermogravimetric analysis (TGA), contact angle measurement, and atomic force microscopy (AFM). Further the blood compatibility of prepared composites was calculated using APTT, PT, and hemolytic assay. SEM analysis of the fabricated scaffolds indicated random morphology of nanofibers with reduced fiber diameter of about  $766 \pm 147$  nm compared to pristine PU control. The FTIR confirms the interaction between PU and castor oil as identified by the formation of hydrogen bond. The developed composite rendered hydrophobic nature owing to increased contact angle and also exhibit higher thermal stability as shown by TGA. The AFM analysis revealed that the surface roughness of the nanocomposites was observed to be improved compared to control. A delay in the activation of clot was noted in activated partial thromboplastin time (APTT) and partial thromboplastin time (PT) assay revealing the anticoagulant nature of the fabricated scaffolds. Moreover, the hemolytic index of developed composites was found to be low indicating the safety of the scaffold in protecting the red blood cells from damage. The present study suggested that newly developed nanocomposite enabled tailoring of desirable characteristics matching for cardiac tissue engineering.

Address correspondence to E-mail: saravana@tdt.edu.vn

## Introduction

Vascular grafts containing biological and synthetic materials have been explored in cardiovascular applications. In the process of bypass or replace the blood vessel, various vascular substitutes were utilized and they resulted in stenosis by disease processes or trauma [1, 2]. The autografts, allografts, or xenografts from saphenous veins or radial arteries were the classical biological grafts used in cardiovascular applications. Owing to the necessity of a donor site, the allografts were partial in supply and dimensions. Despite the allografts and xenografts having some advantages like long-term patency and reactivity, the utilization of them in clinical application is limited by high immunogenic response [1, 3]. In bypassing large-diameter blood vessels (>6 mm), the synthetic grafts such as expanded polytetrafluoroethylene (ePTFE) or Dacron (polyethylene terephthalate fiber), have been used in replacement [1, 4, 5]. On the other hand, small-diameter synthetic grafts showed high failure rates due to thrombosis, stenosis, and occlusion [6–8]. Hence, the fabricated scaffolds should possess the essential qualities like thromboresistant and anticoagulant nature in order to prevent the graft failure [9]. The fabricated scaffold comes in direct contact with red blood cells and it should not induce any damage to the red blood cells. Thromboresistant properties are assessed by the measurement of activated partial thromboplastin time and prothrombin time. These two time points are the good indicators of intrinsic and extrinsic pathways, respectively. Hemolytic percentage may serve as a yard stick for estimating the damage to red blood cells [10].

Tissue-engineered vascular scaffolds make use of natural or synthetic materials to fabricate small arterial substitutes incorporated with endothelial and smooth muscle cells [11–13]. However, the tissue-engineered vascular scaffolds having poor porosity, the infiltration of cells into the scaffold is a great challenge in designing and also showed poor mechanical properties compared with native blood vessels. Recently, electrospinning technology has been promulgated as a substitute for fabricating vascular scaffolds. The electrospinning was used to control the composition, geometry, and mechanical properties of vascular scaffolds, and it could fabricate fibrous matrices with nanoscale dimension which can be substitute for vascular grafts [1].

Electrospinning technique is most versatile and cost effective method for fabricating nanofibers based scaffolds. It involves applying high voltage to polymer melts which is drawn into nanofibers at the collector end. The utilization of electrospinning for biomedical application was performed only in last decade even though the apparatus was invented 100 years ago [14]. Polyurethane is one of the commonly used polymer in the fabrication of tissue-engineered scaffolds and through electrospinning technique the fabrication of nanofibers from PU is easy and make them one of the widely electrospun polymer for medical application. In this research, the polyurethane used to fabricate the nanofibers was tecoflex EG80A which is a polyether-based medical-grade PU. Polyurethane (PU) polymer was used in making nanofibers because it possesses good barrier properties and oxygen permeability which allows cells to proliferate more and suitable for tissue regeneration [15].

The reinforcement used in this study was castor oil. Castor oil is a vegetable oil obtained by pressing the seeds of castor oil plant (*Ricinus Communis*) [16]. Castor oil is colorless to very pale yellow liquid with distinct taste and odor once first ingested. The boiling point of castor oil is 313 °C, and its density is 961 kg/m<sup>3</sup>. It contains triglyceride which is approximately 90% of fatty chains are ricinoleates and other components were oleate and linoleates [17]. The castor oil and its derivatives are used in food and preservative, medicine, manufacturing of soaps, lubricants, hydraulic and brake fluids, paints, dyes, coatings, inks, pharmaceuticals, etc. [18]. Moreover, recent studies suggested that castor oil possess antioxidant nature [19, 20] which provides supports to cells and helps in adhesion and proliferation for the regeneration of new tissue. Diez-Pascual et al. developed wound healing bionanocomposites based on castor oil blended with chitosan and ZnO nanoparticles. It was found that the castor oil scaffold posed no toxicity effect on fibroblast cells and also exhibited faster wound closure rate compared to gauze control [21]. In another work, Ganji et al. studied the cardiomyocyte cells proliferation in polyurethane/gold nanocomposite scaffolds blended with castor oil. It was observed that the castor-incorporated scaffold showed increased cardiomyocyte cells proliferation and has favored new tissue growth [22]. In this work, castor oil is incorporated with pristine PU using a single-step electrospinning process for scaffold

fabrication in cardio vascular applications. Further, physicochemical characterization along with the blood compatibility of the developed nanocomposite will be performed to evaluate the suitability of this scaffold.

## Materials and methods

Tecoflex EG-80A medical-grade thermoplastic polyurethane (PU) was purchased from LubriZol, USA. N, N-dimethylformamide (DMF) was supplied by Merck Millipore, Germany. The commercially available castor oil was obtained locally. The chemicals, phosphate-buffered saline (PBS, Biotech Grade) and sodium chloride physiological saline (0.9% w/v), were supplied by Sigma-Aldrich, Malaysia. The reagents utilized in APTT and PT assay such as rabbit brain activated cephaloplastin, calcium chloride (0.025 M), and thromboplastin (Factor III) were obtained from Diagnostic Enterprises, India.

### Preparation of nanocomposite

To prepare the polymer solution first 480 mg of PU beads were dissolved in 6 ml of DMF followed by magnetic stirring for 24 h at room temperature to obtain a homogenous solution of concentration 8% (w/v). Then 400  $\mu$ l of castor oil was mixed with 4.6 ml of DMF to make 8% v/v solution and stirred for 1 h minimum to obtain a homogenous solution. Finally, the PU–castor oil nanocomposite was prepared by slowly adding castor oil solutions in PU at a ratio of 8:2 under rigorous stirring for 60 min.

### Fabrication of PU and nanocomposite scaffolds

Pure PU nanofiber and PU/castor oil nanocomposite was fabricated using electrospinning technique. The prepared solutions of PU and composite was injected inside the plastic syringe of 10 ml with 18-G stainless steel needle and attached to the syringe pump (SP20, NFiber). Then NFiber high-voltage unit was utilized to supply the voltage for electrospinning apparatus to make nanofibers. The fine nanofibers were obtained and collected on a static drum collector covered with aluminum foil. After several attempts, the PU was successfully electrospun at a flow rate of 1.0 ml/h

with an applied voltage of 10 kV. Since the addition of castor oil has reduced the viscosity of the nanocomposite solution so the flow rate and voltage were changed to 0.50 ml/h and 7 kV, respectively, to obtain a steady stream of the polymer solution. The collector distance was 16 cm which was constantly maintained for both samples. The deposited nanofibrous mesh was detached carefully from the collector and dried at room temperature for 24 h.

### Physicochemical characterization

#### Scanning electron microscopy (SEM) micrographs

The morphology of the electrospun PU and the castor oil nanocomposites fibers were studied using a Hitachi Tabletop SEM unit (TM3000). The developed samples were gold-coated before obtaining the photomicrographs. The diameter size distribution in the developed membranes was examined using Image J (National Institutes of Health, Bethesda, MD) software by measuring 150 individual fibers randomly in six micrographs. Then, the mean fiber diameter with the standard deviation was computed using Image J software.

#### Attenuated total reflectance Fourier transform infrared spectroscopy (ATR-FTIR) analysis

The characteristics of peaks of the electrospun PU and the castor oil nanocomposite were studied was analyzed using the ATR-FTIR unit. In order to identify the IR spectra of PU and castor oil nanocomposite, a small amount of the sample was placed on the sensor surface and the spectra were measured. Meanwhile, the IR spectra of castor oil were obtained by placing a drop of the sensor surface. To investigate the peaks in the spectra each sample were recorded over the range of 600–4000  $\text{cm}^{-1}$  at 32 scans per minute and averaged at the resolution of 4  $\text{cm}^{-1}$ . The ATR crystal used was zinc/selenium which was coupled with the NICOLET IS5 spectrometer. After recording, the spectra were corrected baseline and normalized using Spekwin 32 software to identify the characteristic peaks and differences.

### Contact angle measurement

The contact angle of electrospun PU and the castor oil nanocomposite was calculated using the VCA Optima contact angle measurement unit. For contact angle measurements, the sample of size  $1 \times 5 \text{ cm}^2$  were cut from the mesh for measuring the contact angle. In this setup, the syringe was loaded with the water, and then a droplet of size  $2 \mu\text{l}$  was formed at the tip, and it was carefully placed on the test membrane. Within few seconds, the static image of the liquid deposition within was obtained with the aid of high-resolution video camera. The contact angle measurements of samples were calculated by three different trails, and the manual contact angle was measured through computer integrated software.

### Thermogravimetric analysis

The thermal analysis of electrospun PU and the castor oil nanocomposite was studied using the PerkinElmer TGA 4000 unit. Initially the samples with 3 mg were placed in an aluminium pan, and the experiment was done under a dry nitrogen atmosphere in the temperature range  $30\text{--}1500 \text{ }^\circ\text{C}$  at an ascending rate of  $10 \text{ }^\circ\text{C}/\text{min}$ . Then the remaining weight of the sample was measured at each temperature point and the obtained experimental values were exported in an excel sheet. Then, the TGA curve and the corresponding derivative weight loss curve (DTG) were drawn using OriginPro 8.5 software.

### Atomic force microscopy

Atomic force microscopy was utilized to analyze the sample surface roughness and also to obtain 3D image of the sample surface using JPKSPM data processing software. To perform AFM analysis the sample of size  $1 \times 1 \text{ cm}^2$  were cut from the mesh placed on the AFM equipment (Nanowizard, JPK instruments) and scanned for measuring the surface roughness. In AFM measurement the samples were scanned at room temperature in normal atmosphere. The images were obtained with the scanning size of  $20 \times 20 \mu\text{m}$  and were captured in the medium mode with  $256 \times 256$  pixels. Three measurements were taken at various positions to measure the average surface roughness (Ra).

### Mechanical testing

The mechanical testing was performed in uniaxial load test machine (Gotech Testing Machines, AI-3000) to calculate the tensile strength and young's modulus of the pure PU and prepared nanocomposites. The mechanical test was performed according to the ASTM D638-98. In this experiment, a short segment of electrospun scaffold was cut and was clamped at its cut ends for the axial test. The crosshead speed was  $5 \text{ mm}/\text{min}$ , and the test was stopped when the load decreased by 10% after the onset of failure. The tensile strength and the Young's modulus (modulus of elasticity) were calculated using stress–strain curve at maximum stress.

### Hemocompatibility assessment of the scaffold material

#### Ethical statement and collection of blood samples

All the experimental procedures involved in the handling of blood were approved by Faculty of Biosciences and Medical Engineering, Universiti Teknologi Malaysia with ref no: UTM.J.45.01/25.10/3Jld.2(3). The blood was collected from healthy adults who were educated about the risk and benefits of the blood donation. The blood was collected via venipuncture after getting a signature in the consent form. The collected blood was anticoagulated with acid–citrate–dextrose (ACD) (56 mM sodium citrate, 65 mM citric acid, 104 mM dextrose) at a ratio of 9:1 (blood/citrate). Finally, citrated blood was centrifuged at 3000 rpm for 15 min to extract platelet poor plasma (PPP).

#### Activated partial thromboplastin time (APTT) assay

PU and the PU/castor oil scaffolds were cut into square samples of dimension  $0.5 \times 0.5 \text{ cm}^2$ . For each scaffold, assay was performed in triplicate, and three square samples were introduced into 96-well plates and gently washed with deionized water. The samples were incubated in PBS at  $37 \text{ }^\circ\text{C}$  for 30 min before starting the assay. First,  $50 \mu\text{l}$  of obtained PPP was placed on the sample and incubated for 1 min at  $37 \text{ }^\circ\text{C}$ , and then  $50 \mu\text{l}$  of rabbit brain cephaloplastin

reagent was added and incubated for 3 min at 37 °C. Finally, the reaction mixture was activated by adding 50 µl of CaCl<sub>2</sub> and gently stirred with a sterile steel needle. The time taken for the formation of the white fibrous clot was noted using a chronometer.

### Prothrombin time (PT) assay

Fabricated membrane was cut into square samples as described in the previous subdivision and this test was also performed in triplicate. Samples were washed with deionized water and incubated in PBS for 30 min at 37 °C. To begin the assay, 50 µl of PPP was added to the sample at 37 °C for 1 min, followed by addition of 50 µl of NaCl–thromboplastin reagent (Factor III) and gently mixed with a sterile steel needle until clot formation. The time taken for the clot formation is noted as PT.

### Hemolysis assay

Hemolysis assay was performed in Thermo Scientific Multiskan™ FC (Waltham, MA, USA) to investigate the effect of fabricated membranes with red blood cells. For this both PU and the fabricated samples (1 × 1 cm<sup>2</sup>) were soaked in physiological saline (0.9% w/v) at 37 °C for 30 min. Next they were exposed with a mixture of aliquots of citrated blood and diluted saline (4:5) for 1 h at 37 °C. For constituting positive and negative control, the whole blood was mixed with distilled water (4:5) (complete hemolysis) and also with physiological saline solution, respectively. The exposed samples were retrieved and the mixtures were centrifuged at 3000 rpm for 15 min. The supernatant was aspirated and the absorbance of each sample was recorded at 542 nm which represents red blood cell (RBC) damage. The percentage of hemolysis or hemolytic index was calculated using the formula, [23]

$$\text{Hemolysis ratio (HR)} = \frac{(\text{TS} - \text{NC})}{(\text{PC} - \text{NC})} \times 100$$

where TS, NC, and PC are measured absorbance values of the test sample, negative control, and positive control at 542 nm, respectively.

### Statistical analysis

All experiments were conducted thrice independently. Unpaired *t* test was done to determine

statistical significance. The results obtained from all experiments are expressed as mean ± SD. In case of qualitative experiments, a representative of three images is shown.

## Results and discussion

Biomaterials market share is expected to reach USD 149.17 Billion by 2021 according to recent reports of Markets and Markets. Among these, cardiovascular biomaterials will be occupying the largest share of the biomaterials market in 2016. Hence, there is a good demand for materials for cardiovascular applications. However, the usage of materials in the cardiovascular application (CA) is limited by important characteristics like thrombogenicity and blood compatibility. Similarly, for the material to be used in CA requires proper strength and elasticity. The highlight of this research is the fabricated PU/castor oil composite presents excellent blood compatibility compared to the naïve polymer. Castor oil used in this study can be obtained easily without much difficulty at a trivial cost. Further, tensile strength of the composite developed matches with the mechanical properties of the material used in vascular graft application. The various results of physicochemical and blood compatibility for the fabricated nanocomposites along with pristine PU is discussed below.

The morphology of prepared nanocomposites and pure PU was indicated in SEM image as shown in Fig. 1a and b. The morphology study has revealed that the fibers were finely dispersed and randomly oriented in the matrix. From the SEM image, the polymer PU showed the mean diameter with standard deviation of 1180 ± 106 nm. On the other hand, the prepared PU/castor oil composites showed reduced fiber diameter with mean diameter and standard deviation of 766 ± 147 nm. The fiber diameters distribution curve of pure PU and PU/castor oil composites were shown in Fig. 2a and b. The fiber reduction may be due to increase in conductivity of solution mix during incorporation of castor oil into the pure polymer matrix. Similar results were reported in the research work of polyurethane scaffolds loaded with honey and papaya by Balaji et al. [23]. Kumbhar et al. reported that the fiber diameter of 600–1200 nm was able to support the highest proliferation of fibroblast cells compared with other diametric ranges. They also found that



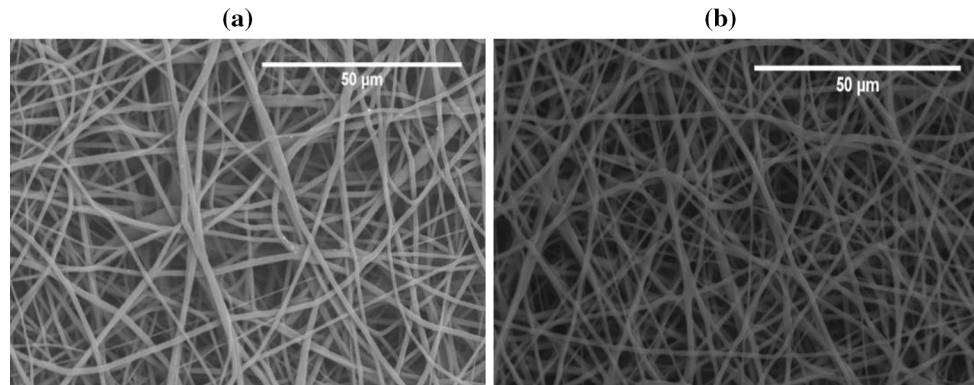
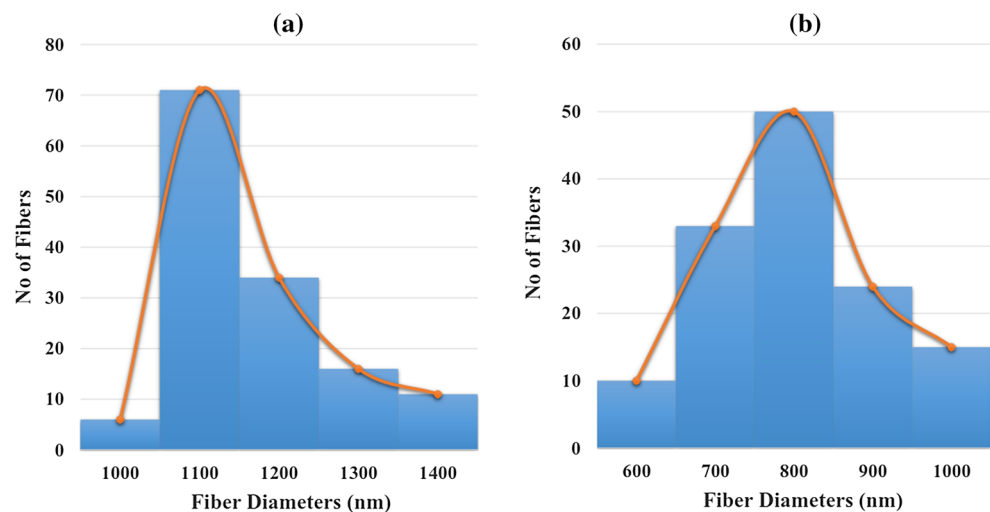


**Figure 1** SEM images of **a** polyurethane membrane, **b** PU/castor oil composites.

**Figure 2** **a** Fiber diameter distributions of a pure PU, **b** PU/castor oil composites.

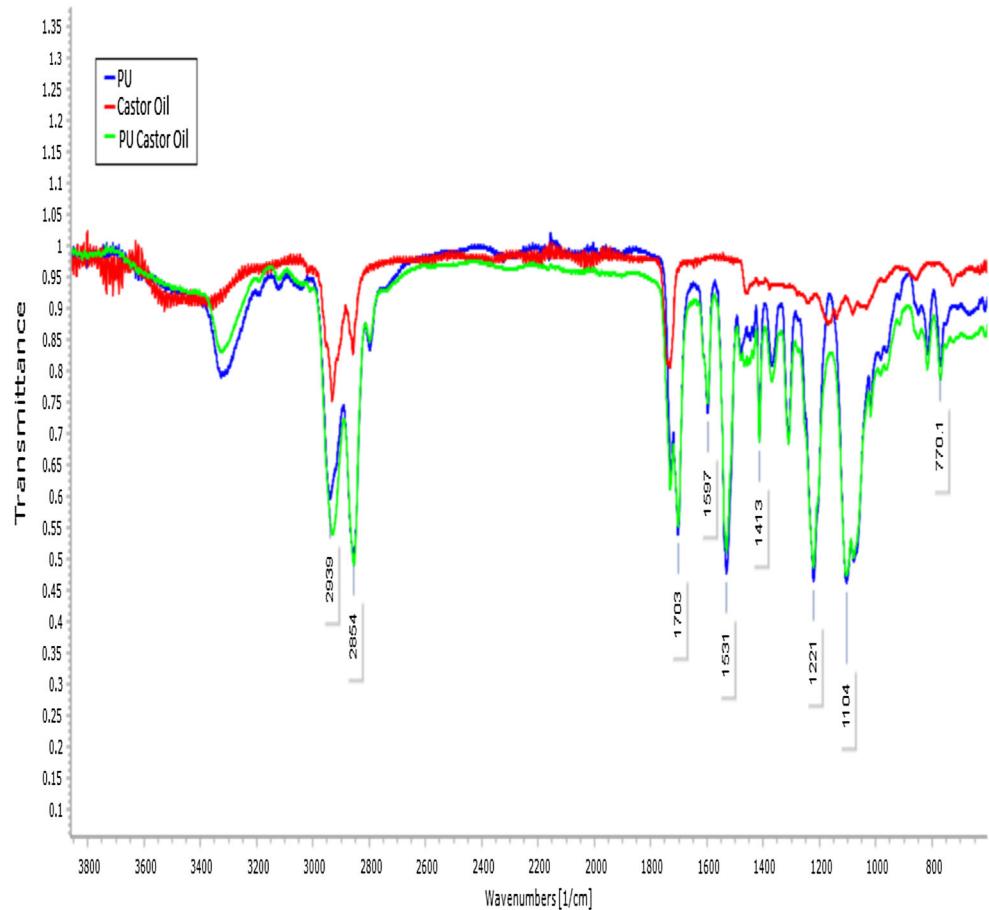


composite of the above said diameter increased the collagen III expression [24]. Hence, our reported fiber diameter values are found to be within this range and may be suitable for supporting the proliferation of fibroblast cells. Osamu et al. fabricated vascular graft using degradable polycaprolactone (PCL) scaffold and suggested that the smaller fiber diameters possess high specific area and porosity, which favors enhanced cell attachment and cell proliferation. Their fabricated PCL scaffold showed reduced fiber diameters and resulted in enhanced number of cell–cell contacts for the regeneration of new tissue growth [25]. Our scaffold fiber diameters showed similar pattern which may favor the enhance cell–cell contacts and proliferation suitable for vascular graft applications.

The functional groups of prepared scaffolds and pure PU were shown in FTIR spectra as in Fig. 3. The peak at  $3323\text{ cm}^{-1}$  denotes the NH stretching of an aliphatic primary amine and peaks at  $1597$  and

$1531\text{ cm}^{-1}$  assisted to vibrations of NH group. The peaks at  $2939$  and  $2854\text{ cm}^{-1}$  shows the  $\text{CH}_2$  stretching and the vibrations of CH was observed at the peak  $1413\text{ cm}^{-1}$ . The C=O stretching of carboxylic groups was identified by twin peak at  $1730$  and  $1703\text{ cm}^{-1}$  and the sharp peaks found at  $1221$ ,  $1104$  and  $770\text{ cm}^{-1}$  indicates the C–O stretching corresponding to alcohol groups [26, 27]. The FTIR spectra of castor oil showed a sharp absorption band frequency at  $2923$  and  $2853\text{ cm}^{-1}$  indicating the aromatic and aliphatic CH stretching, respectively. The C–O stretching was identified by peak at  $1744\text{ cm}^{-1}$ . In PU/castor oil hybrid composites spectra, there were no addition bands present but they showed decreased intensity by the formation of hydrogen bond. In PU/castor oil hybrid composites spectra, there were no addition bands present but they showed decreased intensity by the formation of hydrogen bond. It was reported that the formation of inter-hydrogen bonds between two different

**Figure 3** FTIR analysis of pure PU, castor oil and PU/castor oil composites.



macromolecules were found to stronger than those formed between the molecules of the same polymer [28]. In our developed PU/castor oil nanocomposites, the formation of stronger inter-hydrogen bonds were due to interaction between the CH and CO functional groups in castor oil and PU, respectively. The strong interaction between PU and castor oil is also showed by slight shifting of CH stretching in pure PU from 2939 to 2929  $\text{cm}^{-1}$  and CO stretch from 1730 to 1740  $\text{cm}^{-1}$  in PU/castor oil mats and concluded the presence of castor oil in polyurethane matrix through FTIR analysis [29].

The contact angle measurements of prepared composites PU/castor oil and pure PU are shown below in Table 1. From results obtained, the mean contact angle of PU is found to be  $86^\circ$  whereas the prepared nanocomposites showed contact angle of  $106^\circ$ . It shows that the prepared nanocomposites render hydrophobic surface when the water contact angle exceeded  $90^\circ$ . The contact angle images of prepared PU/castor oil membrane and pure PU are shown in Fig. 4a and b. Some authors Ceylan et al.

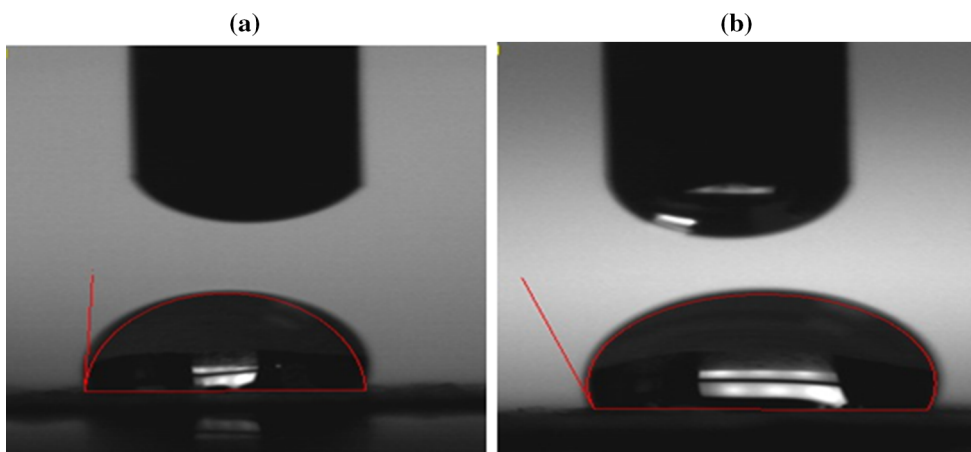
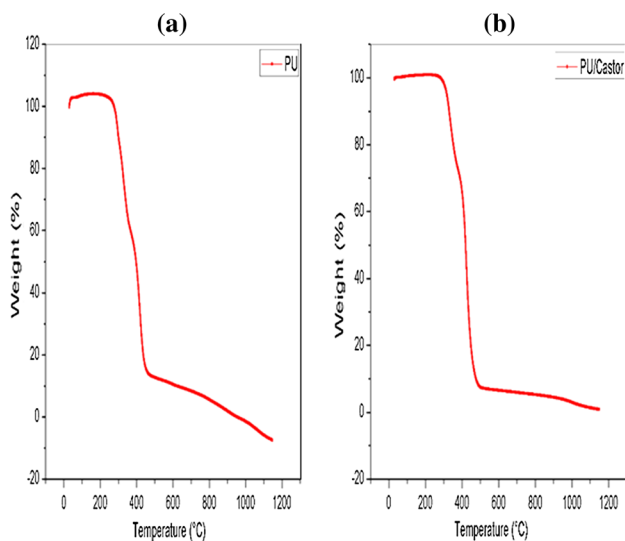
and Cui et al. [30, 31] have reported that that the small fiber diameter generally increases the water contact angle. Our SEM results showed smaller fiber diameter in prepared composites that favors the larger contact angle.

TGA analysis of prepared composite and pure PU samples is shown in Fig. 5a and b. It was observed that the thermal stability of the PU/castor oil hybrids was found to be higher than that of the pure PU. For pure PU, the initial thermal decomposition was found to be  $273^\circ\text{C}$  while for fabricated nanocomposites the onset degradation was found to be  $308^\circ\text{C}$ . Moreover, at  $950^\circ\text{C}$ , the residual weight percentage of the pure PU and prepared nanocomposites was found to be 0.08 and 3.81% indicating the better thermal stability behavior of the composite scaffold. The improved thermal stability could be attributed to the incorporation of castor oil constituents into the pure polymer matrix. The derivative weight loss for pure PU and prepared nanocomposites was found to occur at three stages as shown in Fig. 6a and b. However, the number of stages remains identical for

**Table 1** Contact angle measurement of PU and PU/castor oil composites

S. no	Sample	Average contact angle in degrees
1	Pure polyurethane	86 ± 1.91
2	Polyurethane/castor oil composites	106 ± 1.34*

\* Mean differences were significant compared with pure PU ( $p < 0.05$ )

**Figure 4** Contact angle images of **a** pure polyurethane, **b** polyurethane/castor oil composites.**Figure 5** TGA analysis of **a** pure polyurethane, **b** polyurethane/castor oil composites.

both samples, but their onset and end temperatures were found to be different. For PU, first weight loss is from 273 to 308 °C, the second loss is from 308 to 367 °C, and the third loss from 367 to 453 °C, while for the developed PU/castor oil nanocomposites the first weight loss starts from 308 °C and ends at 325 °C, the second loss from 325 to 378 °C and the third loss from 377 to 485 °C, respectively. Hence, the

results of derivative weight loss indicate the presence of castor oil in the polymer matrix. Gautam et al. developed PCL scaffold blended with gelatin using electrospinning technique for tissue engineering applications. In this study, it was reported that the PCL-blended scaffold showed enhanced thermal stability due to the incorporation of gelatin in the PCL matrix. Since the developed nanocomposites showed enhanced thermal stability, and this might be suitable for tissue engineering applications [32].

Atomic force microscopic measurements of fabricated composite patch and pure PU are shown in Fig. 7a and b. The surface roughness of the pristine PU was found to be 713 nm and for the prepared composite scaffold the surface roughness was found to 1241 nm (Ra), respectively. The incorporated castor oil constituents had increased the surface roughness of polyurethane composites. Mazeyar Parvinzadeh et al. [33] reported the surface properties of polyethylene terephthalate (PET)/clay nanocomposites and had been reported that the addition of clay into polyethylene into PET has improved the surface roughness which is similar to our findings.

Results of tensile testing of pure PU and PU/castor oil nanocomposites are shown Fig. 8a and b. The mechanical testing plays a vital role in influencing cellular morphology, proliferation and differentiation.



**Figure 6** **a** Weight residue percentages of a pure PU, **b** PU/castor oil composites.

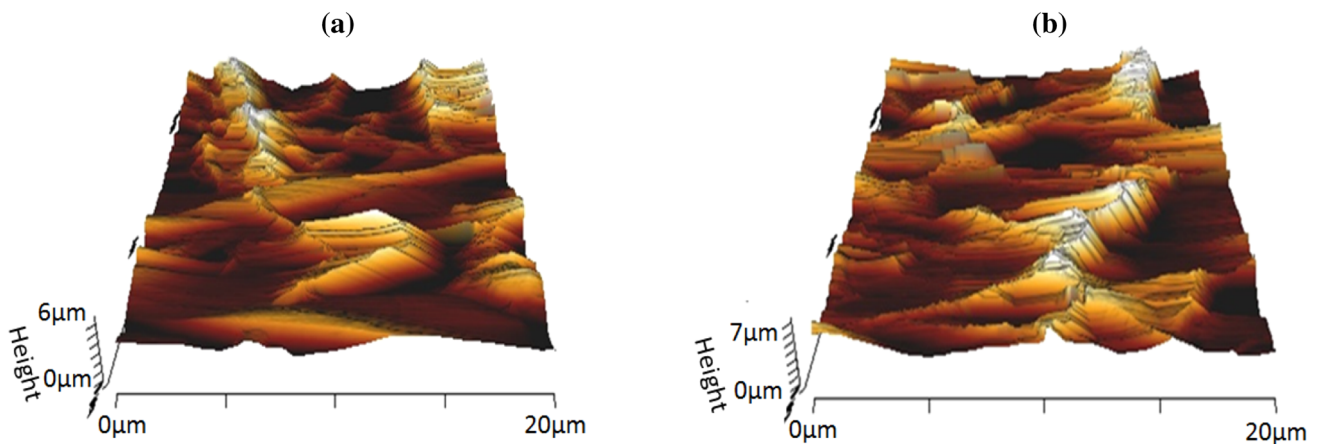
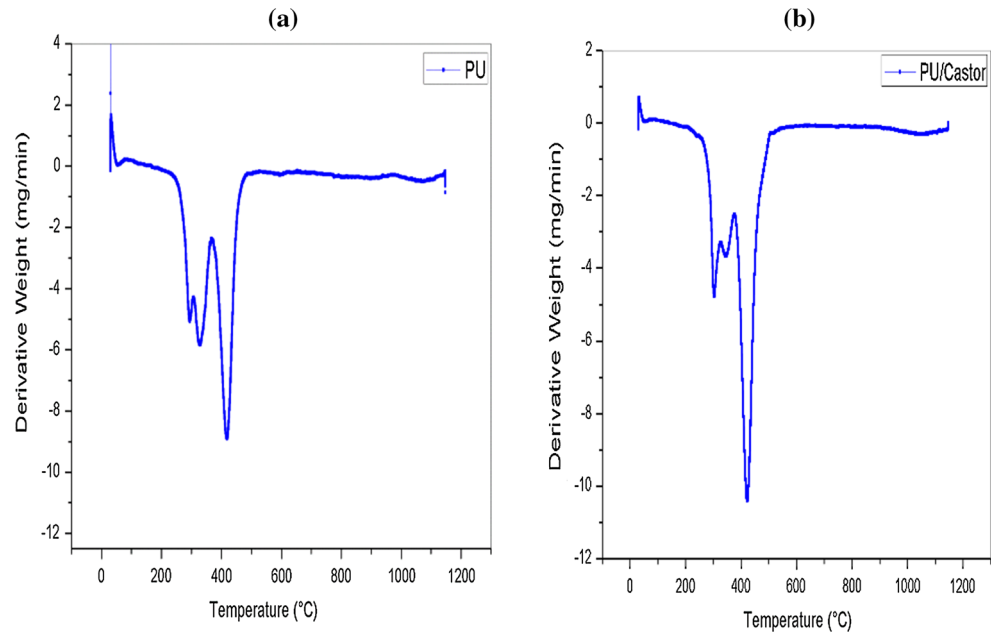


**Figure 7** AFM analysis of **a** pure polyurethane, **b** PU/castor oil composites.

The tensile strength of the electrospun PU scaffolds blended with castor oil was found to be higher than that of the pristine PU. The ultimate tensile strength for prepared nanocomposites was  $5.13 \pm 0.84$  MPa, while for control it was found to be  $4.49 \pm 1.46$  MPa. Moreover, the elastic modulus for the prepared nanocomposites was observed to be 141 MPa, and for the pure PU, it was found to be 95 MPa which was 48% enhancement compared to pure PU. Further, the results have clearly indicated that the castor oil incorporation into the scaffold has improved the tensile properties of the electrospun PU scaffolds. Our obtained results of prepared nanocomposites were compared with tensile strength values of human native blood vessel, aortic valve and cardiac patches.

Hasan et al. reported uniaxial tensile strength value of 3–4 MPa for human saphenous vein in the circumferential direction, whereas for native coronary arteries, tensile strength was reported to be 1.80 MPa [34, 35]. Further, Hasan et al. [36] found the tensile strength value of native aortic valve as 2.6 MPa. Fujimoto et al. [37] prepared cardiac patches based on biodegradable microporous polyester urethane urea (PEUU) for cardiac remodeling and reported that the prepared patches exhibited tensile strength of 0.78 MPa with elongation percentage of 157%. In our study, our calculated tensile strength values were in agreement with the reported values of the above studies thereby making it an interesting candidate for cardiovascular applications.

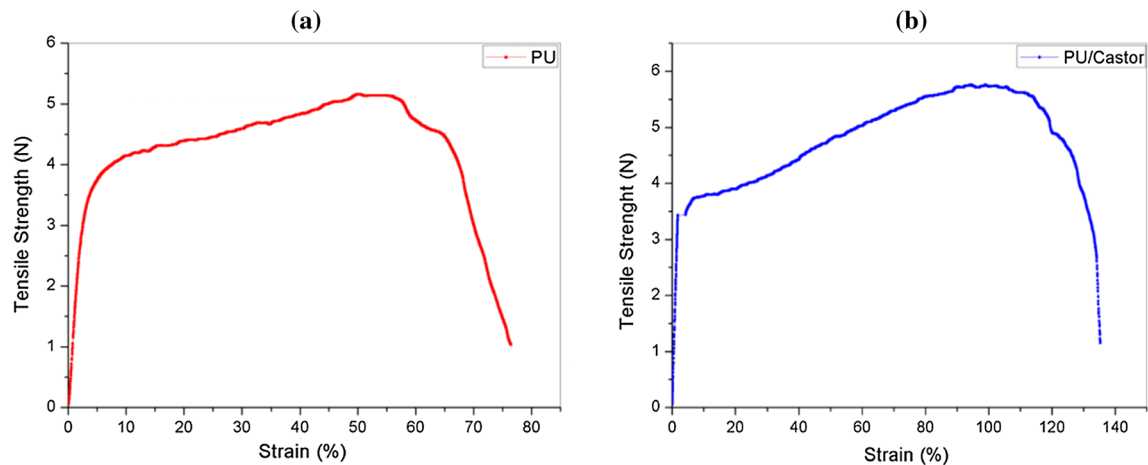


**Figure 8** Tensile strength of **a** pure polyurethane, **b** PU/castor oil composites.

In this work, the APT and PT was employed to investigate the blood clotting and anticoagulant properties of pure PU and PU/castor oil composites. The PT was used to investigate the extrinsic pathway and the APTT was used to investigate the intrinsic pathway, respectively. In this present study, the APTT results revealed that the developed hybrid PU/castor oil composites showed prolonged blood clotting time compared to pure PU membrane. For hybrid scaffolds, the values of APTT were found to  $181 \pm 2.65$  s, while for PU membrane the APTT was observed to be  $157 \pm 5.55$  s as shown in Fig. 9a. The APTT value of fabricated composites clearly shows delayed clotting time suggesting nanocomposite surface better than PU for enhancement in anticoagulant nature. Similarly, in PT assay, the measurement of PT value in fabricated hybrid composites was about  $47 \pm 1.0$  s which was found to be delayed compared to PU ( $38.3 \pm 1.15$  s) as indicated in Fig. 9b. Next, hemolytic assay was done to analyze the safety of the hybrid fabricated scaffold against red blood cells. Hemolysis is very simple and more to reliable method measure blood compatibility of materials. Hemolytic percentage was done by recording the absorbance of obtained supernatant after blood reacts with the composite patch at 542 nm. The measurement of hemolytic assay showed that the absorbance value of PU was found higher compared to PU/castor oil composites indicating lysis of erythrocytes by pristine PU. It was suggested that smaller the hemolysis value, the better would be blood compatibility of the biomaterial. According to ASTM F756-00 (2000) standard, the hemolytic value above 2% was considered as

hemolytic and the value less than 2% was considered as non-hemolytic materials [38]. The fabricated nanocomposite scaffold material displayed a hemolytic percentage of 1.15% indicating non-hemolytic material, while for pure PU the index was observed to 2.7% as shown in Fig. 10. Huang et al. reported that the blood compatibility of a material is influenced by multiple surface characteristics rather than a single factor. The factors influencing the blood compatibility were surface roughness, surface energy, surface tension, surface wettability, and fiber diameters [39]. Ai et al. investigated the surface characteristics and blood compatibility of poly(vinylidene fluoride) (PVDF)/poly(methyl methacrylate) (PMMA) membranes. It was reported that the PVDF/PMMA membranes showed enhanced blood compatibility compared to pure PVDF owing to increase in surface roughness [40]. In another study, Milleret et al. [41] used two polymers namely degarapol and poly(lactic-co-glycolic acid) (PLGA) in developing scaffold with different fiber diameter and found that smaller fiber diameter showed delay in blood clotting indicating better blood compatibility. Chen et al. [42] investigated the blood compatibility of Ti ( $Ta^{+5}$ )O<sub>2</sub> thin films and had reported that the smaller blood/film interfacial tension were partially responsible for the enhancement of the blood compatibility. In another study, Chen et al. prepared carbon/TiO<sub>2</sub> nanocomposite and investigated its blood compatibility. The fabricated nanocomposites exhibited improved anticoagulant function and better blood compatibility due to the hydrophobic nature of the TiO<sub>2</sub> nanowire arrays [43]. Hence, it was difficult to predict which parameters

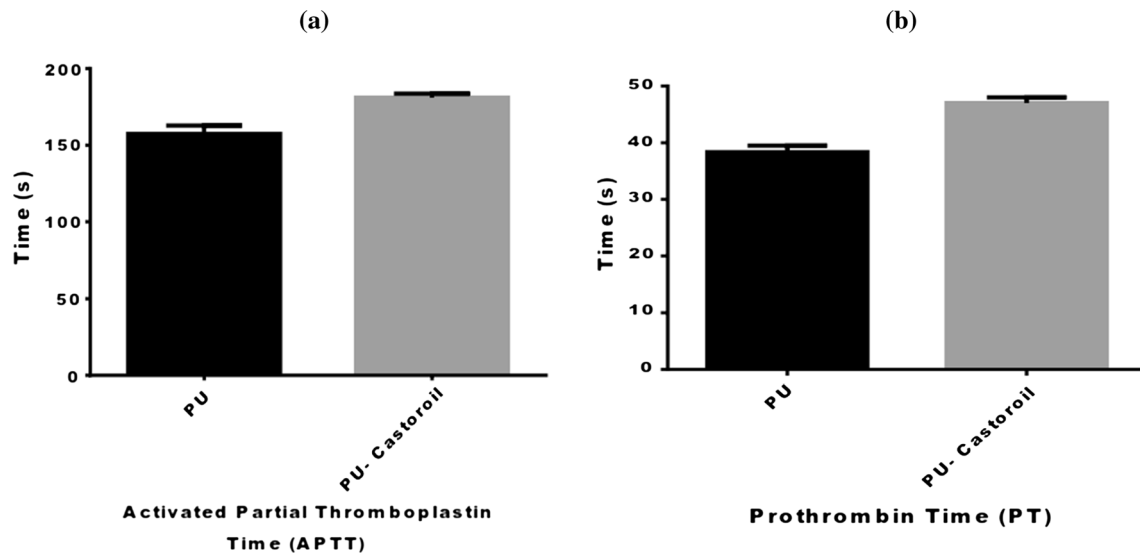


**Figure 9** a APTT and b PT assay of PU and PU/castor oil composites.

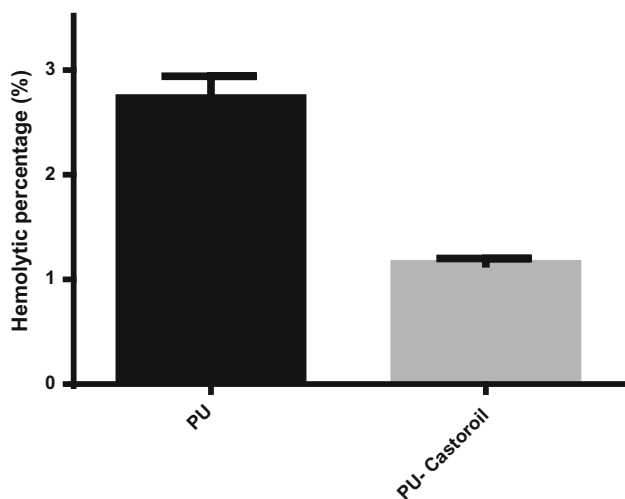


**Figure 10** Hemolysis assay of PU and PU/castor oil composites.

have strong impact on the blood compatibility. The fabricated PU/mustard oil composites showed smaller fiber diameter, hydrophobic nature, and also increased surface roughness which might have contributed to enhanced blood compatibility.

## Conclusions

In this work, the preparation, characterization and blood compatibility of new electrospun nanocomposites based on PU and castor oil were presented. The new designed scaffolds were fabricated using

electrospinning technique. The fabricated composites showed smaller fiber diameter in the range of  $705 \pm 167$  nm, respectively. The FTIR confirms the interaction between PU and castor oil indicated by decrease in intensity of composite scaffolds with the formation of hydrogen bond. The contact angle of polyurethane composites was found to be increased due to castor oil incorporation and also thermal stability was enhanced as spotted in TGA. The surface roughness of PU/castor oil composites was found better and enhanced compared to pure PU. From APTT and PT assay, it was observed that the newly electrospun scaffolds showed delayed activation of blood clot compared to control due to enhanced surface properties. Moreover, compared to pure PU, the electrospun nanocomposites displayed low hemolytic index value indicating the enhanced safety with red blood cells. Hence, the newly fabricated polyurethane scaffold incorporated with castor oil having desirable characteristics such as better physicochemical and blood compatibility which could be applied for future vascular graft applications.

## Acknowledgement

This work was supported by the Ministry of Higher Education Malaysia with the Grant no.Q.J130000.2545.14H59.

## Compliance with ethical standards

**Conflict of interest** The authors declare that they have no conflict of interest.

## References

- [1] Lee SJ, Woo JJ, Jim GJ, Atala A (2007) In vitro evaluation of electrospun nanofiber scaffolds for vascular graft application. *J Biomed Mater Res* 83A:999–1008
- [2] Abbott WM, Callow A, Moore W, Rutherford R, Veith F, Weinberg S (1993) Evaluation and performance standards for arterial prostheses. *J Vasc Surg* 17:746–756
- [3] Bujan J, Garcia-honducilla N, Bellon JM (2004) Engineering conduits to resemble natural vascular tissue. *Biotechnol Appl Biochem* 39:17–27
- [4] Gumpenberger T, Heitz J, Bauerle D, Kahr H, Graz I, Romanin C, Svorcik V, Leisch F (2003) Adhesion and proliferation of human endothelial cells on photochemically modified polytetrafluoroethylene. *Biomaterials* 24:5139–5144
- [5] Xue L, Greisler HP (2003) Biomaterials in the development and future of vascular grafts. *J Vasc Surg* 37:472–480
- [6] Swain TW, Calligaro KD, Dougherty MD (2004) Management of infected aorticprosthetic grafts. *Vasc Endovasc Surg* 38:75–82
- [7] Grego F, Antonello M, Lepidi S, Bonvini S, Deriu GP (2003) Prospective, randomized study of external jugular vein patch versus polytetrafluoroethylene patch during carotid endarterectomy: perioperative and long-term results. *J Vasc Surg* 38:1232–1240
- [8] Nevelsteen A, Lacroix H, Suy R (1995) Autogenous reconstruction with the lower extremity deep veins: an alternative treatment of prosthetic infection after reconstructive surgery for aortoiliac disease. *J Vasc Surg* 22:129–134
- [9] Patterson JT, Gilliland T, Maxfield MW, Church S, Naito Y, Shinoka T, Breuer CK (2012) Tissue-engineered vascular grafts for use in the treatment of congenital heart disease: from the bench to the clinic and back again. *Regen Med* 7(3):409–419
- [10] Amarnath LP, Srinivas A, Ramamurthi A (2006) In vitro hemocompatibility testing of UV-modified hyaluronan hydrogels. *Biomaterials* 27:1416–1424
- [11] Badylak SF, Lantz GC, Coffey A, Geddes LA (1989) Small intestinal submucosa as a large diameter vascular graft in the dog. *J Surg Res* 47:74–80
- [12] Berger K, Sauvage LR, Rao AM, Wood SJ (1972) Healing of arterial prostheses in man: its incompleteness. *Ann Surg* 175:118–127
- [13] Huynh T, Abraham G, Murray J, Brockbank K, Hagen PO, Sullivan S (1999) Remodeling of an acellular collagen graft into a physiologically responsive neovessel. *Nat Biotechnol* 17:1083–1086
- [14] Mokhena TC, Jacobs V, Luyt AS (2015) A review on electrospun bio-based polymers for water treatment. *Polym Lett* 9(10):839–880
- [15] Katti DS, Robinson KW, Ko FK (2004) Bioresorbable nanofiber-based systems for wound healing and drug delivery: optimization of fabrication parameters. *J Biomed Res* 70B:286–296
- [16] Alfred T (2005) Fats and fatty oils, Ullmann's encyclopedia of industrial chemistry. Wiley, Weinheim. doi:10.1002/14356007.a10173
- [17] Aldrich (2003) Handbook of fine chemicals and laboratory equipment. Sigma-Aldrich
- [18] Mutlu H, Meier MA (2010) Castor oil as a renewable resource for the chemical industry. *Eur J Lipid Sci Technol* 112(1):10–30
- [19] Espichan F, Alvarez A, Vela J, Leon K, Santiago J (2010) Effect of gamma radiation on the antioxidant activity of castor oil: Preliminary report. No. INIS-PE-047
- [20] Iqbal J, Zaib S, Farooq U, Khan A, Bibi I, Suleman S (2012) Antioxidant, antimicrobial, and free radical scavenging potential of aerial parts of periploca aphylla and ricinus communis. *ISRN Pharmacol* 2012:563267
- [21] Ganji Y, Li Q, Quabius ES, Böttner M, Selhuber-Unkel C, Kasra M (2016) Cardiomyocyte behavior on biodegradable polyurethane/gold nanocomposite scaffolds under electrical stimulation. *Mater Sci Eng, C* 59:10–18
- [22] Diez-Pascual AM, Diez-Vicente AL (2015) Wound healing bionanocomposites based on castor oil polymeric films reinforced with chitosan-modified ZnO nanoparticles. *Biomacromolecules* 16:2631–2644
- [23] Balaji A, Jaganathan SK, Ismail AF, Rajasekar R (2016) Fabrication and hemocompatibility assessment of novel polyurethane-based bio-nanofibrous dressing loaded with honey and carica papaya extract for the management of burn injuries. *Int J Nanomed* 11:4339–4355
- [24] Kumbar SG, Nukavarapu SP, James R (2008) Electrospun poly(lactic acid-co-glycolic acid) scaffolds for skin tissue engineering. *Biomaterials* 29(30):4100–4107
- [25] Ishii O, Shin M, Sueda T, Joseph P, Vacanti JP (2005) In vitro tissue engineering of a cardiac graft using a degradable scaffold with an extracellular matrix-like topography. *J Thorac Cardiovasc Surg* 130:1358–1363
- [26] Kim SE, Heo DN, Lee JB, Kim JR, Park SH, Jeon SH, Kwon IK (2009) Electrospun gelatin/polyurethane blended nanofibers for wound healing. *Biomed Mater* 4:044106

- [27] Jia L, Prabhakaran MP, Qin X, Ramakrishna S (2014) Guiding the orientation of smooth muscle cells on random and aligned polyurethane/collagen nanofibers. *J Biomater Appl* 29:364–377
- [28] Unnithan AR, Tirupathi PB, Gnanasekaran G, Seenivasan K, Barakat NAM, Jung Y-S, Che-Hun (2012) Emu oil-based electrospun nanofibrous scaffolds for wound skin tissue engineering. *Coll Surf A: Physicochem Eng Asp* 415:454–460
- [29] Tijjing LD, Michael Tom G, Ruelo AA, Pant HR, Park C-H, Kim DW, Kim CS (2012) Antibacterial and superhydrophilic electrospun polyurethane nanocomposite fibers containing tourmaline nanoparticles. *Chem Eng J* 197:41–48
- [30] Cui W, Li X, Zhou S, Weng J (2008) Degradation patterns and surface wettability of electrospun fibrous mats. *Polym Degrad Stab* 93(3):731–738
- [31] Ceylan M (2009) Superhydrophobic behavior of electrospun nanofibers with variable additives. Available at: <http://hdl.handle.net/10057/2535>
- [32] Gautam S, Dinda AK, Mishra NC (2013) Fabrication and characterization of PCL/gelatin composite nanofibrous scaffold for tissue engineering applications by electrospinning method. *Mater Sci Eng C* 33:1228–1235
- [33] Parvinzadeh M, Moradian S, Rashidi A, Yazdanshenas M-E (2010) Effect of the addition of modified nanoclays on the surface properties of the resultant polyethylene terephthalate/clay nanocomposites. *Polym Plast Technol Eng* 49(9):874–884
- [34] Hasan A, Memic A, Annabi N, Hossain M, Paul A, Dokmeci MR, Dehghani F, Khademhosseini A (2014) Electrospun scaffolds for tissue engineering of vascular grafts. *Acta Biomater* 10(1):1–27
- [35] Vorp DA, Schiro BJ, Ehrlich MP, Juvonen TS, Ergin MA, Griffith BP (2003) Effect of aneurysm on the tensile strength and biomechanical behavior of the ascending thoracic aorta. *Ann Thoracic Surg* 75:1210–1214
- [36] Hasan A, Ragaert K, Swieszkowski W, Selimovic S, Paul A, Camci-Unal G, Mofrad MRK, Khademhosseini A (2014) Biomechanical properties of native and tissue engineered heart valve constructs. *J Biomech* 7:1949–1963
- [37] Fujimoto KL, Tobita K, David Merryman W, Guan J, Momoi N, Stolz DB, Sacks MS, Keller BB, Wagner WR (2007) An elastic biodegradable cardiac patch induces contractile smooth muscle and improves cardiac remodeling and function in subacute myocardial infarction. *J Am Coll Cardiol* 49(23):2292–2300
- [38] Fazley M, Elahi GG, Lu W (2014) Hemocompatibility of surface modified silk fibroin materials; a review. *Rev Adv Mater Sci* 38:148–159
- [39] Huang N, Yang P, Leng YX, Chen JY, Sun H, Wang J, Wang GJ, Ding PD, Xi TF, Leng Y (2003) Hemocompatibility of titanium oxide films. *Biomaterials* 24:2177–2187
- [40] Ai F, Li H, Wang Q, Yuan WZ, Chen X, Yang L, Zhao J, Zhang Y (2012) Surface characteristics and blood compatibility of PVDF/PMMA membranes. *J Mater Sci* 47:5030–5040. doi:10.1007/s10853-012-6379-1
- [41] Vincent M, Thomas H, Heike H, Viola V, Daniel E (2012) Influence of fiber diameter and surface roughness of electrospun vascular grafts on blood activation. *Acta Biomater* 8(12):4349–4356
- [42] Chen JY, Leng YX, Tian XB, Wang LP, Huang N, Chu PK, Yang P (2002) Antithrombogenic investigation of surface energy and optical bandgap and hemocompatibility mechanism of Ti(Ta<sup>+5</sup>) O<sub>2</sub> thin films. *Biomaterials* 23:2545–2552
- [43] Chen HL, Luo P, Huang ZY, Chen HP, Chen Min, Chen DH (2013) Preparation and blood compatibility of carbon/TiO<sub>2</sub> nanocomposite. *Diam Relat Mater* 38:52–58